The Cosmic Triangle: Revealing the State of the Universe

Neta A. Bahcall,[1]* Jeremiah P. Ostriker,[1] Saul Perlmutter,[2] Paul J. Steinhardt[3]

The cosmic triangle is introduced as a way of representing the past, present, and future status of the universe. Our current location within the cosmic triangle is determined by the answers to three questions: How much matter is in the universe? Is the expansion rate slowing down or speeding up? And, is the universe flat? A review of recent observations suggests a universe that is lightweight (matter density about one-third the critical value), is accelerating, and is flat. The acceleration implies the existence of cosmic dark energy that overcomes the gravitational self-attraction of matter and causes the expansion to speed up.

As the next millennium approaches, novel technologies are opening new windows on the universe. Whereas previously we relied primarily on fossil evidence found in the local neighborhood of our galaxy to infer the history of the universe, now we can directly see the evolution of the universe over the past 15 billion years, extending as far back as a few 100,000 years after the Big Bang. Thus far, the picture of the past history of the cosmos has altered only slightly; the observations described in this review are consistent with the standard Big Bang model of the expansion of the universe from a hot dense gas, the synthesis of the elements in the first few minutes, and the growth of structure through the gravitational amplification of small initial inhomogeneities. However, the expectation for the future has been dramatically revised. On the basis of the conventional assumption that the universe contains only matter and radiation—the forms of energy we can readily detect—the expectation for the future had been that the expansion rate of the universe would slow continuously because of the gravitational self-attraction of matter. The major issue seemed to be whether the universe would expand forever or ultimately recollapse to a big crunch. Now, the evidence described below is forcing us to consider the possibility that some cosmic dark energy exists that opposes the self-attraction of matter and causes the expansion of the universe to accelerate.

Since the discovery of cosmic expansion by Hubble (*1*) in the 1920s, the standard assumption had been that all energy in the universe is in the form of radiation and ordinary matter (electrons, protons, neutrons, and neutrinos, with mass counting as energy at the rate $E = mc^2$). Over the next several decades, though, theory concerning the stability of galaxies (*2*), observations of the motion of galaxies in clusters (*3, 4*), and observations of the motion of stars and gas surrounding galaxies (*5, 6*) indicated that most of the mass in the universe is dark and does not emit or absorb light (*7, 8*). In the 1980s, the proposal of dark matter found resonance in the inflationary universe scenario (*9–12*), a theory of the first 10^{-30} s designed to address several questions left unanswered by the Big Bang model: Why is the universe so homogeneous and isotropic? Why is the curvature of space so insignificant? And, where did the initial inhomogeneities that give rise to the formation of structure come from (*13–16*)? The standard inflationary theory predicts that the universe is spatially flat; according to Einstein's theory of general relativity, this fixes the total energy density of the universe to equal precisely the critical value, $\rho_c \equiv 3H_0^2/8\pi G \approx 10^{-29}$ g cm^{-3}, where H_0 is the current value of the Hubble parameter and G is Newton's gravitational constant (see Eq. 1). Measurements show that ordinary matter and radiation account for $<10\%$ of the predicted value (*17–19*). Inflation thus seemed to call for dark matter. The observational evidence for dark matter continued to grow, and particle physicists proposed various hypothetical particles, motivated by supersymmetry and unified theories, that could reasonably explain the dark matter. The new consensus model became the cold dark matter picture that predicts that the universe contains primarily cold, nonbaryonic dark matter (*20–22*). Although the total mass density identified by observations still fell short of the critical value (*7, 8, 23, 24*), many cosmologists adopted the critical density model as a working hypothesis, trusting that something would fill the gap.

The past few years have seen signs of another shake-up of the standard model (*25–27*). First, improved observations confirmed that the total mass density is probably less than half of the critical density (*28–30*). At the same time, combined measurements of the cosmic microwave background (CMB) temperature fluctuations and the distribution of galaxies on large scales indicated that the universe may be flat (*26*), consistent with the standard inflationary prediction. The only way to have a low mass density and a flat universe, as expected from the inflationary theory, is if an additional, nonluminous, "dark" energy component dominates the universe today. The dark energy would have to resist gravitational collapse or else it would already have been detected as part of the clustered energy in the halos of galaxies. But, as long as most of the energy of the universe resists gravitational collapse, it is impossible for structure in the universe to form. The dilemma can be resolved if the hypothetical dark energy was negligible in the past and then over time became the dominant energy in the universe. According to general relativity (*31*), this requires that the dark energy have a remarkable feature: negative pressure. This argument (*26*) would rule out almost all of the usual suspects, such as cold dark matter, neutrinos, radiation, and kinetic energy, because they have zero or positive pressure. With the recent measurements of distant exploding stars, supernovae (SNe), the existence of negative-pressure dark energy has begun to gain broader consideration. Using type Ia SNe as standard candles to gauge the expansion of the universe, observers have found evidence that the universe is accelerating (*32, 33*). A dark energy with substantial negative pressure (*26, 34*) will cause the expansion of the universe to speed up, so the SNe observations provide empirical evidence of a dark energy with negative pressure (*32, 35–37*).

The news has brought the return of the cosmological constant, first introduced by Einstein for the purpose of allowing a static universe, with the repulsive cosmological constant delicately balancing the gravitational attraction of matter (*38*). In its present

[1]Princeton University Observatory, Princeton, NJ 08544, USA. [2]Institute for Nuclear and Particle Astrophysics, Ernest Orlando Lawrence Berkeley National Laboratory, Berkeley, CA 94720, USA. [3]Department of Physics, Princeton University, Princeton, NJ 08544, USA.

*To whom correspondence should be addressed. E-mail: neta@astro.princeton.edu

incarnation, the cosmological constant is out of balance, causing the expansion of the universe to accelerate. It can be viewed as a vacuum energy assigned to empty space itself, a form of energy with negative pressure. Cosmologists are familiar with other hypothetical forms of dark energy with negative pressure that can accelerate the universe. In inflationary cosmology, acceleration is caused by a cosmic field (similar to an electric field in the sense that it pervades space and assigns a field value and energy to each point in it) whose kinetic energy is much less than its potential energy (*10, 11*). A different field, with much lower energy, coined "quintessence" (*39*), could account for the acceleration suggested to be observed today. Unlike a cosmological constant, quintessence energy changes with time and naturally develops inhomogeneities that can produce variations in the distribution of mass and the CMB temperature observed today (*39, 40*).

The Cosmic Triangle

According to Einstein's theory of general relativity, the evolution of the universe is determined by the forms of energy it contains and the curvature of space. Einstein's equations can be reduced to a simple form known as the Friedmann equation

$$H^2 = \frac{8\pi G}{3}\rho - \frac{k}{a^2} \qquad (1)$$

On the left-hand side is the Hubble parameter $H = H(t)$, which measures the expansion rate of the universe as a function of time. The current value, H_0, is 65 ± 10 km s^{-1} Mpc^{-1}, where 1 Mpc is 3.26 × 10^6 light-years (*41–43*). The right-hand side contains the factors that determine the expansion rate. The first factor is the energy density ρ (multiplied by Newton's gravitational constant G). The energy density $\rho = \rho(t)$ can have several different subcomponents: a mass density associated with ordinary and dark matter, the kinetic energy of the particles and radiation, the energy associated with fields (such as quintessence), and the vacuum energy density or, equivalently, the cosmological constant. The second term on the right-hand side describes the effect of curvature of space on the expansion of the universe. The curvature constant k can be positive, negative, or zero. The parameter $a = a(t)$, known as the scale factor, measures how much the universe stretches as a function of time. It can be thought of as being proportional to the average distance between galaxies. As the universe stretches, the curvature is diminished, as indicated in Eq. 1. The terms "closed," "open," and "flat" refer, by definition, to the cases of positive, negative, and zero curvature, respectively. It has been common to use the same terms to describe whether the universe will ultimately recollapse, expand forever, or lie on the border between expansion and recollapse. This second use does not necessarily apply if there is vacuum density or quintessence, a point which often causes confusion. For example, if there is vacuum energy, it is possible to have a universe that is closed (positive curvature) but expands forever because the acceleration due to the cosmological constant overcomes the curvature effect (*44*), which would otherwise bring the expansion to a halt and then recollapse.

For simplicity, we will consider a universe that is currently composed of baryonic (ordinary) and dark (exotic) matter, curvature, and vacuum energy (that is, a cosmological constant Λ). The fractional contributions to the right-hand side of the Friedmann equation, which depend on the relative values of the matter density, vacuum energy density ρ_Λ, and curvature, are given the symbols $\Omega_m \equiv 8\pi G\rho_{matter}/(3H^2)$, $\Omega_\Lambda \equiv 8\pi G\rho_\Lambda/(3H^2) \equiv \Lambda/(3H^2)$, and $\Omega_k \equiv -k/(aH)^2$, respectively (*45*). Dividing both sides of Eq. 1 by H^2 yields a simple sum rule

$$1 = \Omega_m + \Omega_k + \Omega_\Lambda \qquad (2)$$

For any other energy component, such as quintessence, a term Ω_Q would be added to the right-hand side of Eq. 2. The sum rule can be represented by an equilateral triangle (Fig. 1). Lines of constant Ω_m, Ω_k, and Ω_Λ run parallel to each of the edges of the equilateral triangle. Every point lies at an intersection of lines of constant Ω_m, Ω_k, and Ω_Λ, such that the sum rule is satisfied. Although Ω_m is nonnegative, the curvature and cosmological constant can be positive or negative.

Inflationary theory (*9–12*) proposes that the universe underwent a brief epoch of extraordinary expansion during the first 10^{-30} s after the Big Bang, which ironed out the

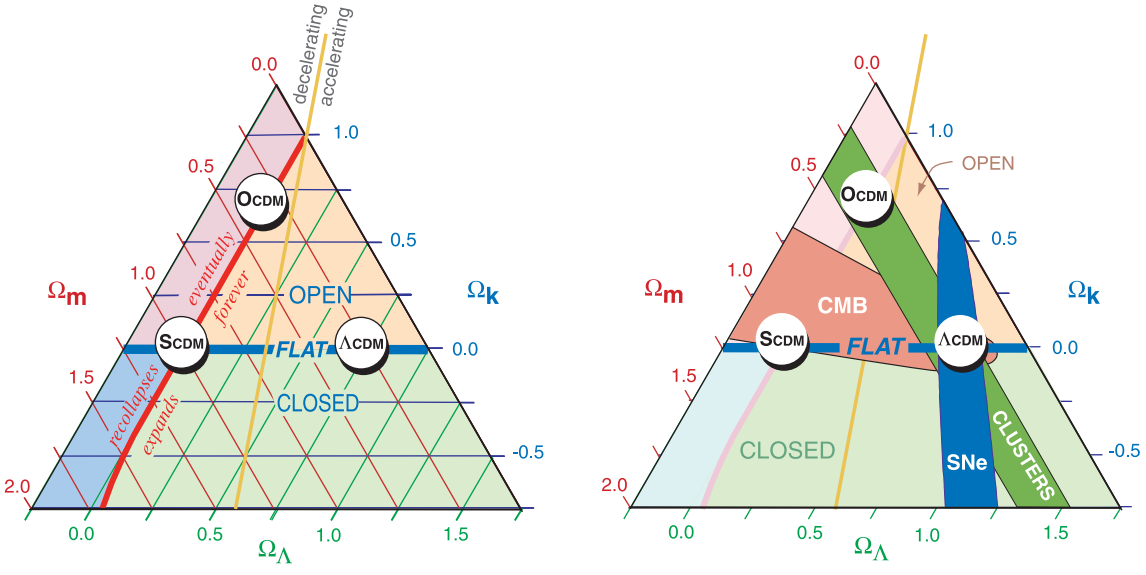

Fig. 1 (left). The Cosmic Triangle. This triangle represents the three key cosmological parameters (Ω_m, Ω_Λ, and Ω_k), where each point in the triangle satisfies the sum rule $\Omega_m + \Omega_\Lambda + \Omega_k = 1$. The horizontal line (marked "FLAT") corresponds to a flat universe ($\Omega_m + \Omega_\Lambda = 1$), separating an open universe from a closed one. The red line, nearly along the $\Lambda = 0$ line, separates a universe that will expand forever (approximately $\Omega_\Lambda > 0$) from one that will eventually recollapse (approximately $\Omega_\Lambda < 0$). And the yellow, nearly vertical line separates a universe with an expansion rate that is currently decelerating from one that is accelerating. The locations of three key models are highlighted: SCDM, dominated by matter ($\Omega_m = 1$) and no curvature or cosmological constant; flat (ΛCDM), with $\Omega_m = 1/3$, $\Omega_\Lambda = 2/3$, and $\Omega_k = 0$; and OCDM, with $\Omega_m = 1/3$, $\Omega_\Lambda = 0$, and $\Omega_k = 2/3$. (The variant tilted TCDM model is identical in its position to SCDM.) **Fig. 2 (right). The Cosmic Triangle Observed.** This triangle represents current observational constraints. The tightest constraints from measurements at low redshift (clusters, including the mass-to-light method, baryon fraction, and cluster abundance evolution), intermediate redshift (SNe), and high redshift (CMB) are shown by the three color bands (each representing 1σ uncertainties). Other tests that we discuss are consistent with but less constraining than the constraints illustrated here. The cluster constraints indicate a low-density universe, the SNe constraints indicate an accelerating universe, and the CMB measurements indicate a flat universe. The three independent bands intersect at a flat model with $\Omega_m \approx 1/3$ and $\Omega_\Lambda \approx 2/3$; the model contains a cosmological constant or other dark energy.

curvature, setting $\Omega_k = 0$. If the curvature is zero, that is, the universe is flat, then the sum rule reduces to $\Omega_m + \Omega_\Lambda = 1$ (Fig. 1, "FLAT" line). The yellow line in Fig. 1 indicates the division between models in which the universe expansion is currently decelerating versus models in which it is accelerating. The competition between the decelerating effect of the mass density and the accelerating effect of the vacuum energy density can be understood from Einstein's equation for the stretching of the scale factor $a(t)$

$$\ddot{a} = -\frac{4\pi G}{3}(\rho + 3p)a \qquad (3)$$

where p is the pressure associated with whatever energy is contained within the universe. If the universe contains ordinary matter and radiation, then $\rho + 3p$ is positive, and the expansion decelerates ($\ddot{a} < 0$). However, exotic components like vacuum energy and quintessence (*39, 40*) have sufficient negative pressure to make $\rho + 3p$ negative, inducing cosmic acceleration.

Finally, models of special interest have been highlighted in Fig. 1; they form a nearly equilateral triangle of their own. The standard cold dark matter model (SCDM), the simplest possibility, has $\Omega_m = 1$ and no curvature or vacuum component. The model assumes a "scale-invariant" spectrum of initial density fluctuations, a spectrum in which the magnitude of the inhomogeneity is the same on all length scales, as predicted by standard inflationary cosmology (*13–16*). A model that better fits observations and retains the simple condition of $\Omega_m = 1$ is the tilted cold dark matter model (TCDM), in which the fluctuation spectrum is tilted so that the average inhomogeneity increases with the length scale, unlike the standard inflationary prediction. The open cold dark matter model (OCDM) has low mass density and no vacuum component; the best fit version has a mixture of one-third matter density and two-thirds curvature (but no vacuum energy) with a spectrum that is tilted the opposite way from the TCDM model (the inhomogeneity decreases as the length scale increases). As an example of a dark energy plus cold dark matter model (ΛCDM), a current "best estimate" model, we will consider a mixture of two-thirds vacuum density (or Λ) and one-third matter density (but no curvature) and the standard untilted spectrum predicted by inflationary theory. The parameters for each of the four models (Table 1) were chosen to fit each type of model to the current observational constraints discussed below. All the models (and our analysis) assume the standard inflationary prediction that the density fluctuations are Gaussian and adiabatic (that is, matter and radiation fluctuate spatially in the same manner) (*13–16*), which agree with current observations. The age of the universe (Table 1, Age) is consistent with the most recent estimates of the ages of the oldest stars (*46, 47*).

The models may be distinguished observationally by answering three fundamental questions: Is there enough matter to close (flatten) the universe? Is the expansion rate accelerating, providing evidence for a new dark energy? And, is the universe curved? In the next sections, we describe a series of independent tests aimed at addressing these three questions. The best constraint for each question is represented as a strip in the plot in Fig. 2. Together, these constraints determine our location in the cosmic triangle plot and, thereby, the past and future evolution of the universe.

Is There Enough Mass to Close the Universe?

The possibility of a low-mass-density universe ($\Omega_m < 1$) has gained support for over a decade (*7, 8, 23, 24, 26, 28–30*). The determination of the universe's mass density is currently the best studied of the three cosmological parameters and is supported by a number of independent measurements. Although each observation has its strengths, weaknesses, and assumptions, they all indicate that $\Omega_m < 1$.

Mass-to-light method. One of the oldest and simplest techniques for estimating the total mass of the universe entails a two-step process: first, determine the average ratio of the mass to the emitted light of the largest systems possible; then, multiply this ratio by the total measured luminosity density of the universe. This totals up all the mass associated with light to the largest scales. Rich clusters of galaxies are the largest (1 to 2 Mpc in radius) and most massive (2×10^{14} to 10×10^{14} solar masses within 1 Mpc) bound systems known for which mass has been reliably measured. Cluster mass can be inferred from three independent methods: the galaxy motion within the cluster, the temperature of the hot intracluster gas, and the gravitational lensing by the cluster mass (the distortion of background galaxies' images by the cluster's gravitational potential). There is agreement among these independent estimators. The mean cluster mass-to-light ratio (M/L), about 200 ± 70 times the M/L for the sun, indicates that there is a great deal of dark matter within clusters (*28, 29*). Nevertheless, even if we assume that all light in the universe is emitted from objects that have as much mass per unit of light as clusters, the total mass would not be sufficient to close the universe. Multiplying M/L by the observed luminosity density, one obtains $\Omega_m = 0.2 \pm 0.1$ (*7, 28, 29*). Recent studies of the dependence of M/L on scale indicate that M/L is nearly constant on large scales ranging up to supercluster size (10 Mpc), suggesting that no additional dark matter is tucked away on large scales (*28, 48*).

Baryon fraction method. An independent method of estimating the mass of the universe, also based on rich clusters, entails measuring the ratio of the baryonic to total mass in clusters (*49, 50*). Because clusters form through gravitational collapse, they scoop up the mass over a large volume of space so that the ratio of baryons to total matter in the collapsed cluster should be representative of the cosmic average to within 20% (*51, 52*). The Big Bang model of primordial nucleosynthesis constrains the baryon density to be $\Omega_b = 0.045 \pm 0.0025$ (based on the cosmic abundance of helium and deuterium and using $H_0 = 65$ km s^{-1} Mpc^{-1}) (*17–19*). Thus, if one can measure the average baryon ratio in the universe, Ω_b/Ω_m, it can be used with the known Ω_b to determine Ω_m. A cluster's baryon ratio can be determined from the baryonic mass in the cluster [obtained by measuring the x-ray emission from the hot intracluster gas and adding the mass of the stars (*49, 53*)] divided by the total cluster mass. The baryon ratio is found to be $\Omega_b/\Omega_m \approx 0.15$, much larger than the 0.045 value expected if $\Omega_m = 1$ (*49–52*). The observed ratio corresponds to a mass density of $\Omega_m = 0.3 \pm 0.1$. If some baryons are ejected from the cluster during gravitational collapse, as suggested by cosmological simulations (*51, 52*), or if some baryons are bound in nonluminous objects such as rocks or planetary-sized objects, then the actual value of Ω_m is lower than this estimate.

Cluster abundance and its evolution. Another feature of rich clusters that constrains Ω_m is the number density of clusters as a function of cosmic time (or redshift) (*30, 54–58*). Rich clusters are the most recently formed gravitationally bound objects in the universe. The ob-

Table 1. The basic parameters for the four cold dark matter (CDM) models considered in this paper. Ω_m, Ω_Λ, and Ω_k are the ratio of the mass, vacuum energy, and curvature to the critical density. H_0 is the Hubble parameter (in km s^{-1} Mpc^{-1}). The tilt measures how the amplitude of the inhomogeneity in initial density perturbations changes with length scale; tilt equal to unity means that the amplitude is scale invariant, which is the inflationary prediction. The age of the universe is in 10^9 years. ΛCDM is in best agreement with current observations (Fig. 2).

Model	Ω_m	Ω_Λ	Ω_k	H_0	Tilt	Age
Cosmological const. (ΛCDM)	1/3	2/3	0	65	1	14.1
Open (OCDM)	1/3	0	2/3	65	1.3	12.0
Standard (SCDM)	1	0	0	50	1	13.0
Tilted (TCDM)	1	0	0	50	0.7	13.0

served present-day ($z \approx 0$) cluster abundance provides a constraint on the normalization of the power spectrum of density fluctuations—the seeds that created the clusters—on the relevant cluster scales (*24, 54, 59*). The ΛCDM and OCDM models are consistent with the observed cluster abundance at $z \approx 0$. SCDM, however, when normalized to match the observed fluctuations in the CMB, produces too many clusters at all redshifts (Fig. 3) (*24, 55, 59, 60*). The TCDM model preserves $\Omega_m = 1$ and more nearly fits the present-day cluster abundance (Figs. 3 and 4).

The evolution of cluster abundance with redshift breaks the $z \approx 0$ degeneracy among the models (*30, 54–56*). The $\Omega_m < 1$ models (ΛCDM and OCDM) predict relatively little change in the number density of rich clusters as a function of redshift because, due to the low matter density, hardly any structure growth has occurred since $z \approx 1$. For the $\Omega_m = 1$ TCDM model, structure has been growing steadily, and rich clusters could only have formed recently; the number density of rich clusters at $z \simeq 0.5$ to 1 is predicted to be exponentially smaller than today. The observation of even one massive cluster at a high redshift ($z > 0.6$) suffices to rule out the $\Omega_m = 1$ model. In fact, three clusters have been observed already (Fig. 3), suggesting a low-density universe, $\Omega_m = 0.25^{+0.15}_{-0.1}$ (1σ) (*30*). A caveat for this method is that it assumes that the initial spectrum of density perturbations is Gaussian, as predicted by inflation, which has not yet been confirmed observationally [but, see (*61*)] on the cluster scales.

Mass power spectrum. The mass power spectrum (Fig. 4) measures the degree of inhomogeneity in the universe's mass distribution on different distance scales. Beginning from a cosmological model, the mass power spectrum depends on the initial spectrum of inhomogeneities (for example, the stretched-out quantum fluctuations predicted by inflation), the recent creation of new perturbations, and how those inhomogeneities have evolved over time (which depends on the cosmological parameters). Existing measurements of the present-day abundance of galaxy clusters constrain the mass inhomogeneity on the smallest scale for which the power spectrum can be reliably interpreted (~10 Mpc). Observations of temperature fluctuations in the CMB across the sky, as measured by the Cosmic Background Explorer (COBE) satellite (*62*), constrain both the amplitude and shape of the spectrum on the largest observable scales (~1000 Mpc).

Galaxy surveys are beginning to probe intermediate scales, from 10 to 1000 Mpc (Fig. 4) (*63, 64*). The theoretical model predicts the distribution of all the mass, whereas observations of galaxies reflect the luminous baryonic matter only. If the luminous matter follows the total mass, the mass distribution is said to be "unbiased." Otherwise, the ratio of overdensity in luminous matter to that in the total mass is termed the "bias." On small scales, the bias may vary with distance scale and local environment. These complications can be avoided by focusing on measurements of the power spectrum on large scales [>10 Mpc (Fig. 4)], where the inhomogeneities are small and the bias is expected to be small (*65, 66*). Although current galaxy measurements are inconclusive, especially given uncertainty in the bias, future surveys, such as the Sloan Digital Sky Survey (*64*), are poised to test the shape of the spectrum on intermediate scales.

Inflation predicts the shape of each spectrum (*13–16*), but it does not predict its normalization (that is, amplitude). The normalization is determined from observations, mainly the observed cluster abundance (on 10-Mpc scales) and the CMB fluctuations (on 1000-Mpc scales). The $\Omega_m = 1$ SCDM model, normalized to the CMB fluctuations on large scales, is inconsistent with the cluster abundance [predicting over 10 times more clusters than observed (Fig. 3)]. SCDM is thus inconsistent with observations (*24, 26, 30, 54, 57, 59, 60*). The model can be forced to approximately agree with the cluster abundance on small scales and the CMB fluctuations on large scales by tilting the power spectrum (by ~30%) from its standard shape. This tilted variant of the SCDM model, TCDM, is thus nearly consistent with both constraints. The power spectra of the ΛCDM and OCDM models can be normalized so that they agree with the CMB and cluster observations (with a 30% tilt needed for OCDM). Future observations, on all scales, will greatly improve the power spectrum constraints. This will allow a measurement of Ω_m from the shape of the spectrum; currently, this measurement suggests a low value of Ω_m, but with large uncertainty.

Overall estimate of Ω_m. Other methods, such as statistics of gravitational lensing, large-scale velocities (*67*), and measurements of the CMB anisotropy, place additional constraints on Ω_m in combination with other parameters and assumptions; although less constraining, these also suggest a low-mass density (*36, 37*). The net result is represented by the "clusters" band (1σ) in the cosmic triangle of Fig. 2. It is remarkable that a single value of Ω, $\Omega_m \simeq 1/3$, is consistent with so many diverse observations.

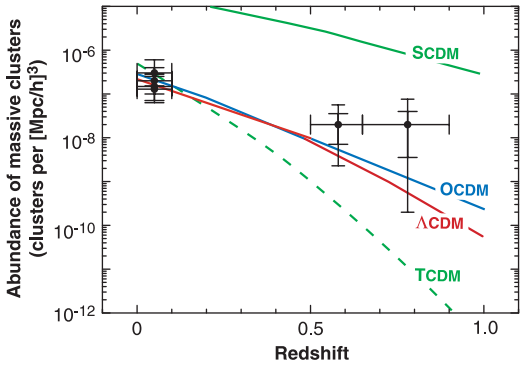

Fig. 3. The evolution of cluster abundance as a function of redshift is compared with observations for massive clusters (>10^{15} solar masses within a radius of 2 Mpc, assuming H_0 = 65 km s^{-1} Mpc^{-1}) (*30*). Only the ΛCDM and OCDM fit well the observed cluster abundance at $z \approx 0$ (see also Fig. 4), although the TCDM fits much better than the SCDM model. All four models are normalized to the CMB fluctuations on large scales. The observational data points (*30*) (with 1σ and 2σ error bars) show only a slow evolution in the cluster abundance, consistent with low-Ω_m models and inconsistent with $\Omega_m = 1$.

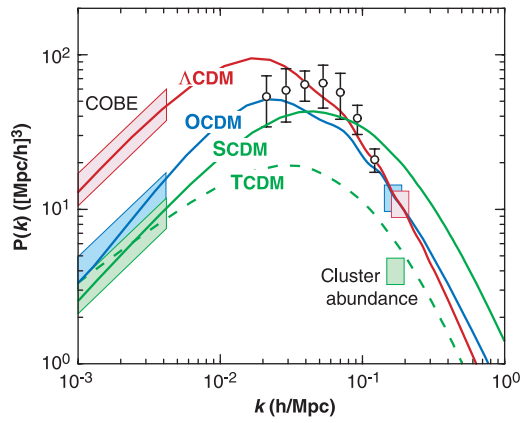

Fig. 4. The mass power spectrum represents the degree of inhomogeneity in the mass distribution as a function of wave number *k*. [The wave number is inversely proportional to the length scale; small scales are to the right (large *k* values), and large scales are to the left (small *k* values).] COBE measurements of the CMB anisotropy (shaded areas on the left) and measurements of cluster abundance at $z \sim 0$ (boxes on the right) impose different quantitative constraints for each model; the constraints have been color-coded to indicate the model to which they apply. All curves are normalized to the CMB fluctuations on large scales (that is, curves are forced to pass through the COBE areas on the left). The COBE-normalized SCDM model significantly overshoots the cluster constraint (green box on the right). The data points with open circles and 1σ error bars represent the APM galaxy redshift survey (*63*); if one assumes bias, then this set of points can be shifted downward to match the model, but the shape of the spectrum suggested by the data is unchanged.

Is the Universe's Expansion Accelerating?

Changes in the cosmic expansion rate can be studied with the observed brightness-redshift

relation. A set of standard candles (objects of known luminosity) spread throughout the universe is used to determine the relation between distance and redshift. The distance d_L is determined by comparing the known luminosity L to the flux observed at Earth f_{obs} and invoking the inverse-square law ($f_{obs} = L/4\pi d_L^2$). By studying standard candles at different observed fluxes, we study objects whose light was emitted at different cosmic times. The redshift z of the object measures the expansion of the universe since that time.

For relatively nearby standard candles, the distance d_L is a simple linear function of redshift, as given by the Hubble relation of the expanding universe, $H_0 d_L = cz$, where c is the speed of light. However, the linear relation is only an approximation. If we study standard candles that are farther away, the nonlinearities in the d_L-z relation become important because the universe's expansion may be decelerating or accelerating. The results are most sensitive to the difference between Ω_m (which decelerates the expansion) and Ω_Λ (which accelerates the expansion) and are rather insensitive to the curvature Ω_k.

Type Ia SNe are currently the best candidates for standard candles. They have the advantage of being bright and can be seen at cosmic distances. As a class, type Ia SNe are not all identically luminous, but examination of nearby SNe indicates that they may be converted into reliable distance indicators by calibrating them according to the time scale of their brightening and fading (*68, 69*). Two efforts are under way to collect data on the redshift, luminosity, and light curves of distant SNe: the Supernova Cosmology Project (SCP) (*32, 69, 70*) and the High-*Z* Supernova Search (HZS) (*33, 71, 72*). Observations and analyses of ~50 type Ia SNe at $z = 0.3$ to 0.9 have been published and calibrated with a comparable number of nearby SNe (*73, 74*) at $z \lesssim 0.1$.

The results of the two studies show that the distant SNe are fainter and thus more distant than expected for a decelerating universe (Fig. 5). It appears that the expansion rate is accelerating, indicating the existence of dark energy with negative pressure, such as Ω_Λ. The best fit results (Fig. 2) can be approximated by the linear combination $0.8\Omega_m - 0.6\Omega_\Lambda = -0.2 \pm 0.1$ (1σ) (*32, 75*). For a flat universe ($\Omega_m + \Omega_\Lambda = 1$), the best fit values are approximately $\Omega_m = 0.25 \pm 0.1$ and $\Omega_\Lambda = 0.75 \pm 0.1$ (1σ) for the combined results of the SCP team (*32*) and the two analyses of the HZS team (*33*). These values are in excellent agreement with the Ω_m results discussed in the previous section. In particular, all flat $\Omega_m = 1$ models, which are identical in their d_L-z predictions, are formally ruled out at the 8σ level.

The caveats for this test are possible uncertainties in the cross comparison of the near and distant SNe. Distant SNe are calibrated with nearby SNe, assuming that the light-curve time scale accounts for any relevant evolution of type Ia SNe. Although known evolutionary and dust obscuration effects have been taken into account, there remains the concern that there are additional evolutionary or dust effects at large redshift that have not been noted before; this is being investigated with observations of distant and nearby SNe. The current results suggest that the expansion of the universe is accelerating, indicating the existence of a cosmological constant or dark energy.

Gravitational lensing due to accumulations of matter along the line of sight to distant light sources provides another potentially sensitive measure of our position in the cosmic triangle. These measures can be used in two ways. The first method uses the abundance of multiply imaged sources such as quasars, lensed by intervening galaxies (*76–79*). The probability of finding lensed images is directly proportional to the number of galaxies (lenses) along the path and thus to the distance in light-years to the source. This distance (for fixed H_0) increases dramatically for a large value of Λ. The age of the universe and the distance to the galaxy become large in the presence of Ω_Λ because the universe has been expanding for a longer time (compared with an $\Omega_m = 1$ case); therefore, more lenses are predicted if $\Omega_\Lambda > 0$. With this method, an upper limit of $\Omega_\Lambda < 0.75$ (95% confidence limit) has been obtained (*76–79*), marginally consistent with the SNe results. The caveats of this method include its sensitivity to uncertainties in the number density and lensing cross section of the lensing galaxies and the number density of distant faint quasars. A second method is lensing by massive clusters of galaxies (*80, 81*). Such lensing produces widely separated lensed images of quasars and distorted images of background galaxies. The observed statistics of this lensing, when compared with numerical simulations, rule out the $\Omega_m = 1$ models (*80, 81*) and set an upper bound of $\Omega_\Lambda < 0.7$ (*81*). The limit is sensitive to the resolution of the numerical simulations, which are currently improving.

Is the Universe Curved?

The curvature of the universe can be measured from the highest redshift cosmological test—the CMB. The CMB power spectrum provides a measure of the inhomogeneity in matter and energy at $z \approx 1000$, corresponding to a few 100,000 years after the Big Bang. The power spectrum is the root-mean-square fluctuation in the CMB temperature (the temperature "anisotropy") as a function of the angular scale expressed as an integer multipole moment l. A given l value corresponds roughly to an angle of π/l radians. Each cosmological model produces a distinguishable CMB temperature anisotropy fingerprint (*82, 83*). On large angular scales (small l values), the CMB spectrum probes inhomogeneities that span distances so large (~1000 Mpc) that neither light nor any other interaction has had time to traverse or modify them.

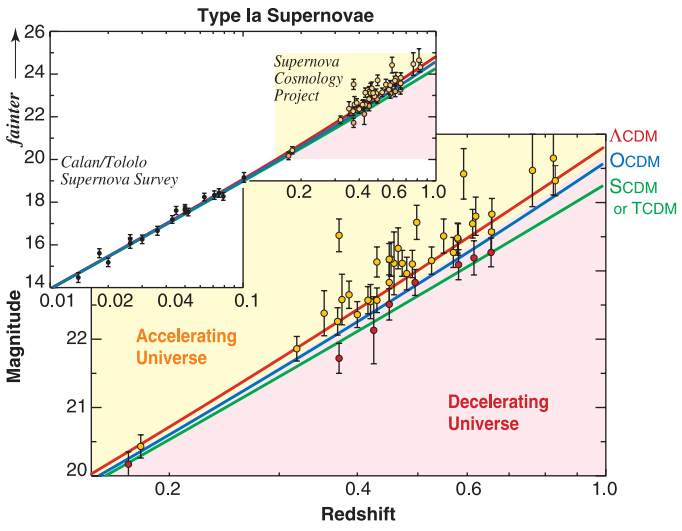

Fig. 5. Supernovae as standard candles. The relation of observed brightness (in logarithmic units of "magnitude") versus redshift for type Ia SNe observed at low redshift by the Calan-Tololo Supernova Survey and at high redshift by the SCP is presented (with 1σ error bars) and compared with model expectations. (Brighter is down, and dimmer is up.) (All $\Omega_m = 1$ flat models yield identical predictions in this method; thus, TCDM is identical to SCDM.) The strong gravitational pull exerted by $\Omega_m = 1$ models (such as TCDM or SCDM), decelerates the expansion rate of the universe and produces an apparent "brightening" of high-redshift type Ia SNe, whereas the effect of a cosmological constant accelerating the expansion rate (as in ΛCDM) is seen as a relative "dimming" of the distant type Ia SNe caused by their larger distances. The plot on the lower right shows a close-up view of the expected deviations between the models as a function of redshift. The background color (and shading of the data points) indicates the region for which the universe's expansion would accelerate (yellow) or decelerate (red) for $\Omega_m \approx 0.2$. (Higher values of Ω_m would extend the yellow accelerating-universe region farther down on this plot.) Similar results were found by the HZS team (*33*). The results provide evidence for an accelerating expansion rate.

These inhomogeneities are a direct reflection of the initial spectrum (for example, as created by inflation). If the models predict an untilted or a tilted spectrum, then the CMB anisotropy spectrum has a plateau that is flat or tilted, respectively. On small angular scales ($<1°$ or $l > 200$), the anisotropy spectrum has peaks and valleys created by the small-scale inhomogeneities; on these scales, there has been sufficient time for light to traverse them and for the matter to respond gravitationally to the density fluctuation. The hot gas of baryons and radiation begin a series of acoustic oscillations in which matter and radiation are drawn by gravity into regions of high density and then rebound because of the finite pressure of the gas. On scales corresponding to the "sound horizon" (the maximum distance that pressure waves can travel from the beginning of the universe up to the time the CMB is emitted), the mass has had time to undergo maximum collapse around the dense regions so as to produce maximum anisotropy but has not had time to rebound. Hence, a peak in the power spectrum is anticipated on the angular scale corresponding to the sound horizon, and this should be the peak with the largest angular scale (smallest l value). An interesting feature is that the physical length corresponding to the sound horizon is relatively insensitive to the cosmological model. The angular scale that it subtends on the sky depends on the overall curvature of space; the curvature distorts the path of light so that the sound horizon appears bigger or smaller on the sky, depending on whether the curvature is positive or negative. If the universe is flat, the sound horizon subtends ~1° on the sky (resulting in a power spectrum peak near $l \approx 200$), whereas the angular size is smaller in a curved open model [resulting in a peak near $l \approx 200/(\Omega_m + \Omega_\Lambda)^{1/2}$] (*84*).

The CMB anisotropy was detected by the COBE satellite in 1992 (*85*), followed by a series of ground- and balloon-based experiments (*86–91*). Here, we have selected published experiments that measure at several frequencies (to eliminate foreground sources) and that have been cross-correlated with other measurements (Fig. 6). In the next few years, there will be a sequence of ground- and balloon-based experiments culminating in the NASA Microwave Anisotropy Probe and the ESA PLANCK satellite missions, which will produce all-sky temperature maps with a resolution of a few arc minutes. These improved maps will do much more than measure the position of the first acoustic peak and, thereby, the curvature; by measuring the detailed shape of the plateau and a sequence of peaks with very high precision, they will confirm (or refute) the basic underlying cosmological scenario and, if confirmed, will help to determine additional cosmological parameters, such as Ω_m, Ω_Λ, Ω_b, H_0, and others (*92, 93*). The best fit parameter region derived from the current CMB results (Fig. 2) is consistent with a flat universe, although the uncertainty is large. This analysis assumes that the initial fluctuations are adiabatic, as predicted by the standard inflationary theory and as assumed in our four models. If they are not, this will be apparent from future CMB observations, and a different means can be used to extract the curvature from CMB data.

If the universe is flat and the matter density is less than the critical density, then there must be some form of nonclustering dark energy. In that case, as discussed in the introduction, the only way to form the observed large-scale structure is if its pressure is negative, which guarantees that its density was negligible in the past when structure formed. This conclusion is consistent with the evidence suggesting that the universe is accelerating, which can only occur with a substantial negative pressure component.

The Cosmic Triangle: Past, Present, and Future

The current state of the universe can be surmised from the answers to the three questions posed above. The most precise measurements of the mass (using clusters), the acceleration (using SNe), and the curvature (using the CMB) each confine the universe to a strip in the cosmic triangle plot (Fig. 2). All three strips overlap at the ΛCDM model with approximately $\Omega_m = 1/3$, $\Omega_\Lambda = 2/3$, and $\Omega_k = 0$ (*36, 37*). Zero curvature is consistent with inflation.

The verification and refinement of these conclusions will take place in the next few years through experiments that are already under way and will hopefully settle some of the questions that have challenged cosmologists for most of the 20th century. However, new cosmological challenges will take their place. Establishing inflation as the source of the fluctuations that seeded galaxy formation requires tests of the shape, Gaussianity, and gravitational wave component of the primordial power spectrum (*82, 94–96*). As estimates of the cold dark matter density become more precise, it becomes even more imperative that its composition be identified. A host of candidates are suggested by particle physics models (*97*). The leading candidates at present are the axion (*98*) and the lightest, stable, supersymmetry partner particles, such as the photino and higgsino (*99*). [Recent measurements of atmospheric and solar neutrinos show that the neutrino has a small mass, but the mass is probably too small to be important cosmologically (*100*).]

However, it is the acceleration of the universe that raises the most provocative and profound issues. The acceleration may be caused by a static uniform vacuum density (or cosmological constant) or by a dynamical form of evolving inhomogeneous dark energy (quintessence) (*39, 40*). Distinguishing between the two cosmologically is important because it informs

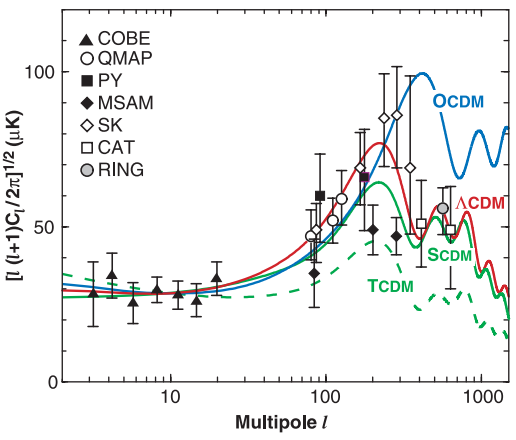

Fig. 6. The CMB temperature anisotropy is presented as a function of angular scale. The multipole l corresponds roughly to an angular scale of π/l radians. Flat models ($\Omega_m + \Omega_\Lambda = 1$) produce an acoustic peak at $l = 200$ (about 1° on the sky). Open models have a peak that is shifted to smaller scales (larger l values). (The height of the peak depends on additional parameters, including Ω_m, Ω_Λ, Ω_b, H_0, and tilt; here, we use the model values from Table 1.) The observational data points (with 1σ error bars) include the COBE measurements on large scales (small l values) and other published, multifrequency ground- and balloon-based observations [QMAP (*86*), PY (*87*), MSAM (*88*), SK (*89*), CAT (*90*), and RING (*91*)].

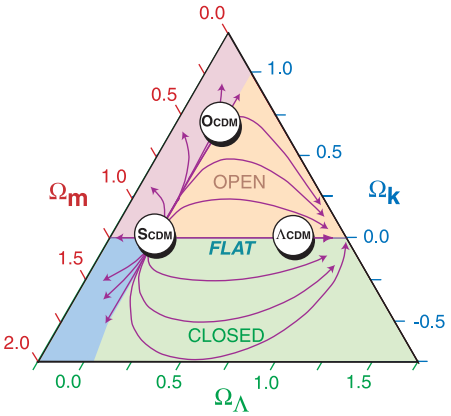

Fig. 7. The Cosmic Triangle: Past, Present, and Future. The past and future of the universe are represented by various trajectories in the cosmic triangle. The trajectories, which originate from near $\Omega_m = 1$ (an unstable equilibrium point matching the approximate condition of the universe during early structure formation), indicate the path traversed in the triangle plot as the universe evolves. For the current best fit ΛCDM model, the future represents a flat accelerating universe that expands forever, ultimately reaching $\Omega_m \rightarrow 0$ and $\Omega_\Lambda \rightarrow 1$.

us of what kind of new fundamental physics may be required to explain our universe. Promising approaches include measurements of SNe, CMB anisotropy, and gravitational lensing (*32, 35–37*). Special initial conditions are required for the vacuum energy possibility because it remains constant while the matter density decreases over 100 orders of magnitude as the universe expands. To have a vacuum energy density only a factor of 2 greater than the matter density today, it would have to have been exponentially small in comparison to the matter density in the early universe. A major motivation for proposing quintessence is that its interactions can cause its energy to naturally adjust itself to be comparable to the matter density today without special initial conditions (*101*).

Acceleration also affects our projection for the future fate of the universe, which can also be represented in a cosmic triangle plot (Fig. 7). As the universe evolves, Ω_m, Ω_k, and Ω_Λ change at different rates, while maintaining a total value of unity, according to the sum rule. Possible trajectories to the future (Fig. 7) show that $\Omega_m = 1$ is an unstable fixed point and $\Omega_\Lambda = 1$ is a stable fixed point. If $\Omega_m < 1$ today and there is any bit of added dark energy, then we are ultimately careening towards a flat $\Omega_m \rightarrow 0$ ($\Omega_\Lambda \rightarrow 1$) universe in which the matter is spreading infinitesimally thin, leaving behind only an inert vacuum energy. If the vacuum energy (or quintessence) is unstable, this fate may be averted.

As the current millennium ends, the past history and the present state of the universe are making themselves known. Determining the long-term fate of the universe will require an understanding of the fundamental physics underlying the dark energy, one of the grand challenges for the millennium to come.

References and Notes

1. E. Hubble, *Proc. Natl. Acad. Sci. U.S.A.* **15**, 168 (1929).
2. J. P. Ostriker and P. J. E. Peebles, *Astrophys. J.* **186**, 467 (1973).
3. F. Zwicky, *Helv. Phys. Acta* **6**, 110 (1933); S. Smith, *Astrophys. J.* **83**, 23 (1936).
4. N. A. Bahcall, *Annu. Rev. Astron. Astrophys.* **15**, 505 (1977).
5. H. W. Babcock, *Lick Obs. Bull.* **19**, 41 (1939); M. Schwarzschild, *Astron. J.* **59**, 273 (1954).
6. V. Rubin and W. K. Ford, *Astrophys. J.* **159**, 379 (1970); M. S. Roberts and A. H. Rots, *ibid.* **186**, L95 (1973).
7. J. P. Ostriker, J. P. E. Peebles, A. Yahil, *ibid.* **193**, L1 (1974).
8. V. Trimble, *Annu. Rev. Astron. Astrophys.* **25**, 423 (1987); A. Dekel, D. Burstein, S. D. M. White, in *Critical Dialogues in Cosmology*, N. Turok, Ed. (World Scientific, Singapore, 1997).
9. A. H. Guth, *Phys. Rev. D* **23**, 347 (1981).
10. A. D. Linde, *Phys. Lett. B* **108**, 389 (1982).
11. A. Albrecht and P. J. Steinhardt, *Phys. Rev. Lett.* **48**, 1220 (1982).
12. For an introduction to inflationary cosmology, see A. H. Guth and P. J. Steinhardt, in *The New Physics*, P. Davies, Ed. (Cambridge Univ. Press, Cambridge, 1989), pp. 34–60.
13. J. Bardeen, P. J. Steinhardt, M. S. Turner, *Phys. Rev. D* **28**, 679 (1983).
14. A. H. Guth and S.-Y. Pi, *Phys. Rev. Lett.* **49**, 1110 (1982).
15. A. A. Starobinskii, *Phys. Lett. B* **117**, 175 (1982).
16. S. W. Hawking, *ibid.* **115**, 295 (1982).
17. T. P. Walker, G. Steigman, D. N. Schramm, K. Olive, H. S. Kang, *Astrophys. J.* **376**, 51 (1991).
18. S. Burles and D. Tytler, *ibid.* **499**, 699 (1998); *ibid.* **507**, 732 (1998).
19. D. N. Schramm and M. S. Turner, *Rev. Mod. Phys.* **70**, 303 (1998).
20. P. J. E. Peebles, *Astrophys. J.* **263**, L1 (1982); *ibid.* **277**, 470 (1984).
21. S. D. M. White, C. S. Frenk, M. Davis, G. Efstathiou, *ibid.* **313**, 505 (1987).
22. "Cold" matter means that the kinetic energy is much less than the mass energy. Nonbaryonic means that the matter is not made of "ordinary" matter such as protons and neutrons (called baryons by particle physicists).
23. J. R. Gott, J. E. Gunn, D. N. Schramm, B. M. Tinsley, *Astrophys. J.* **194**, 543 (1974).
24. N. A. Bahcall and R. Cen, *ibid.* **398**, L81 (1992).
25. L. A. Kofman, N. Y. Gnedin, N. A. Bahcall, *ibid.* **413**, 1 (1993).
26. J. P. Ostriker and P. J. Steinhardt, *Nature* **377**, 600 (1995).
27. L. Krauss and M. S. Turner, *Gen. Rel. Grav.* **27**, 1135 (1995).
28. N. A. Bahcall, L. M. Lubin, V. Dorman, *Astrophys. J.* **447**, L81 (1995).
29. R. G. Carlberg *et al.*, *ibid.* **462**, 32 (1996).
30. N. A. Bahcall and X. Fan, *Proc. Natl. Acad. Sci. U.S.A.* **95**, 5956 (1998); *Astrophys. J.* **504**, 1 (1998).
31. A simple computation in general relativity shows that the ratio of the dark energy density to the matter density is $a(t)^{-3p/\rho}$, where p is the pressure, ρ is the energy density of the dark energy, and $a(t)$ is the scale factor of the universe at a given time. As one extrapolates back in time in an expanding universe, the scale factor a gets smaller. So, if $p > 0$, the ratio increases in the past, the matter density would never have dominated, and structure would never have formed. If $p < 0$ (negative pressure), the ratio decreases in the past, the matter density would have dominated, and structure would have formed.
32. S. Perlmutter *et al.*, available at http://xxx.lanl.gov/abs/astro-ph/9812473; S. Perlmutter *et al.*, *Astrophys. J.*, in press (available at http://xxx.lanl.gov/abs/astro-ph/9812133).
33. A. G. Riess *et al.*, *Astron. J.* **116**, 1009 (1998).
34. J. P. E. Peebles, *Astrophys. J.* **284**, 439 (1984).
35. P. M. Garnavich *et al.*, *ibid.* **509**, 74 (1998).
36. L. Wang, R. Caldwell, J. P. Ostriker, P. J. Steinhardt, in preparation (available at http://xxx.lanl.gov/abs/astro-ph/9901388).
37. S. Perlmutter, M. S. Turner and M. White, in preparation (available at http://xxx.lanl.gov/abs/astro-ph/9901052).
38. A. Einstein, *Sitzungsber. Preuss. Akad. Wiss.* **1917**, 142 (1917).
39. R. R. Caldwell, R. Dave, P. J. Steinhardt, *Phys. Rev. Lett.* **80**, 1582 (1998).
40. N. Weiss, *Phys. Lett. B* **197**, 42 (1987); B. Ratra and J. P. E. Peebles, *Astrophys. J.* **325**, L17 (1988); C. Wetterich, *Astron. Astrophys.* **301**, 32 (1995); J. A. Frieman *et al.*, *Phys. Rev. Lett.* **75**, 2077 (1995); K. Coble, S. Dodelson, J. Frieman, *Phys. Rev. D* **55**, 1851 (1995); P. G. Ferreira and M. Joyce, *Phys. Rev. Lett.* **79**, 4740 (1997); *Phys. Rev. D* **58**, 023503 (1998).
41. W. L. Freedman, J. R. Mould, R. C. Kennicutt, B. F. Madore, *Int. Astron. Union Symp. 183* (1998) (available at http://xxx.lanl.gov/abs/astro-ph/9801080).
42. G. A. Tammann, in *General Relativity*, 8th Marcel Grossman Symposium, Hebrew University, Jerusalem, 22 to 27 June 1997; T. Piran, Ed. (World Scientific, Singapore, in press) (available at http://xxx.lanl.gov/abs/astro-ph/9805013).
43. S. T. Myers, J. E. Baker, A. C. S. Readhead, E. M. Leitch, *Astrophys. J.* **485**, 1 (1997).
44. The vacuum energy can overtake the matter density and curvature and prevent recollapse in a closed universe because the different components evolve differently with time: The matter density decreases as $1/a^3$, the curvature decreases as $1/a^2$, and the cosmological constant remains constant, thus eventually dominating the energy of the universe.
45. It is conventional to write $\Omega_i = \rho_i/\rho_c$, where ρ_c is the critical density, $\rho_c \equiv 3H^2/8\pi G = 10^{-29}$ g cm^{-3} (for the present value of $H_0 = 65$ km s^{-1} Mpc^{-1}). ρ_c is proportional to H^2, which decreases with time.
46. B. Chaboyer, P. Demarque, P. J. Korman, L. M. Krauss, *Astrophys. J.* **494**, 96 (1998).
47. M. Salaris and A. Weiss, *Astron. Astrophys.* **335**, 943 (1998).
48. N. Kaiser *et al.*, *Astrophys. J.*, in press (available at http://xxx.lanl.gov/abs/astro-ph/9809268).
49. S. D. M. White, J. F. Navarro, A. Evrard, C. Frenk, *Nature* **366**, 429 (1993).
50. D. White and A. C. Fabian, *Mon. Not. R. Astron. Soc.* **273**, 72 (1995).
51. R. Cen and J. P. Ostriker, *Astrophys. J.* **429**, 4 (1994); L. M. Lubin, R. Cen, N. A. Bahcall, J. P. Ostriker, *ibid.* **460**, 10 (1996).
52. M. Arnaud and A. E. Evrard, *Mon. Not. R. Astron. Soc.*, in press (available at http://xxx.lanl.gov/abs/astro-ph/9806353).
53. M. Fukugita, C. J. Hogan, P. J. E. Peebles, *Astrophys. J.* **503**, 518 (1998).
54. V. Eke, S. Cole, C. S. Frenck, *Mon. Not. R. Astron. Soc.* **282**, 263 (1996).
55. N. A. Bahcall, X. Fan, R. Cen, *Astrophys. J.* **485**, L53 (1997).
56. R. G. Carlberg, S. M. Morris, H. K. C. Yee, E. Ellingson, *ibid.* **479**, L19 (1997).
57. J. P. Henry, *ibid.* **489**, L1 (1997).
58. L. Wang and P. J. Steinhardt, *ibid.* **508**, 483 (1998).
59. S. D. M. White, G. Efstathiou, C. S. Frenk, *Mon. Not. R. Astron. Soc.* **262**, 1023 (1993).
60. J. P. Ostriker, *Annu. Rev. Astron. Astrophys.* **31**, 698 (1993).
61. W. A. Chiu, J. P. Ostriker, M. A. Strauss, *Astrophys. J.* **494**, 479 (1998).
62. E. F. Bunn and M. White, *ibid.* **480**, 6 (1997).
63. J. Peacock, *Mon. Not. R. Astron. Soc.* **284**, 885 (1997).
64. J. E. Gunn, M. Carr, C. Rockosi, M. Sekiguchi, *Astron. J.* **116**, 3048 (1998).
65. J. N. Fry, *Astrophys. J.* **461**, L65 (1996).
66. M. Tegmark and P. J. E. Peebles, *ibid.* **500**, L79 (1998).
67. The motions of galaxies and clusters on large scales provide a promising method in constraining the mass density of the universe (because the motions are a response to the gravitational force due to the mass density fluctuations). Current estimates of Ω_m from this method exhibit a large scatter, with results ranging from $\Omega_m = 0.2$ to 1 [for example, review by M. Strauss and J. Willick, *Phys. Rep.* **261**, 271 (1995)]. Therefore, no accurate constraint has been placed so far on Ω_m. Similar large uncertainties exist in the reports of large-scale bulk motions of galaxy clusters [T. Lauer and M. Postman, *Astrophys. J.* **425**, 418 (1994); J. Willick *et al.*, available at http://xxx.lanl.gov/abs/astro-ph/9812470; M. J. Hudson *et al.*, available at http://xxx.lanl.gov/abs/astro-ph/9901001].
68. M. M. Phillips, *Astrophys. J.* **413**, L105 (1993); A. G. Riess, W. H. Press, R. P. Kirshner, *ibid.* **438**, L17 (1995); *ibid.* **473**, 88 (1996).
69. S. Perlmutter *et al.*, *ibid.* **483**, 565 (1997).
70. S. Perlmutter *et al.*, in *Thermonuclear Supernovae*, P. Ruiz-Lapuente, R. Canal, J. Isern, Eds. (Kluwer, Dordrecht, Netherlands, 1997), pp. 749–758.
71. P. Garnavich *et al.*, *Astrophys. J.* **493**, L53 (1998).
72. B. P. Schmidt *et al.*, *ibid.* **507**, 46 (1998).
73. M. Hamuy *et al.*, *Astron. J.* **109**, 1 (1995); *ibid.* **112**, 2391 (1996).
74. A. G. Riess *et al.*, *ibid.* **117**, 707 (1999).
75. A. Goobar and S. Perlmutter [*Astrophys. J.* **450**, 14 (1995)] discuss the dependence on redshift of the particular linear combination of Ω_m and Ω_Λ determined by the SNe measurements and present an approach to obtaining both parameters separately by measuring SNe at a wide range of redshifts.
76. E. L. Turner, J. P. Ostriker, J. R. Gott III, *Astrophys. J.* **284**, 1 (1984).
77. D. Maoz and H.-W. Rix, *ibid.* **416**, 425 (1993).

78. C. S. Kochanek, *ibid*. **453**, 545 (1995); *ibid*. **466**, 638 (1996).
79. E. E. Falco, C. S. Kochanek, J. A. Munoz, *ibid*. **494**, 47 (1998).
80. J. Wambsganss, R. Cen, J. P. Ostriker, E. L. Turner, *Science* **268**, 274 (1995); *Astrophys. J.*, in press (available at http://xxx.lanl.gov/abs/astro-ph/9610096).
81. M. Bartelmann *et al*., *Astron. Astrophys*. **330**, 1 (1998).
82. For an introduction to the CMB power spectrum and its interpretation see P. J. Steinhardt, in *Particle and Nuclear Astrophysics and Cosmology in the Next Millenium*, E. W. Kolb and P. Peccei, Eds. (World Scientific, Singapore, 1995), pp. 51–72.
83. The physics of CMB anisotropy generation is discussed in W. Hu, N. Sugiyama, J. Silk, *Nature* **386**, 37 (1997).
84. M. Kamionkowski, D. N. Spergel, N. Sugiyama, *Astrophys. J.* **426**, L57 (1994).
85. G. F. Smoot *et al*., *ibid*. **396**, L1 (1992); C. L. Bennett *et al*., *ibid*. **464**, L1 (1996).
86. M. J. Devlin *et al*., *ibid*. **509**, L69 (1998); T. Herbig *et al*., *ibid*., p. L73; A. Oliveira-Costa *et al*., *ibid*., p. L77.
87. S. R. Platt *et al*., *ibid*. **475**, L1 (1997).
88. E. S. Cheng *et al*., *ibid*. **488**, L59 (1997).
89. B. Netterfield, M. J. Devlin, N. Jarosik, L. Page, E. L. Wallack, *ibid*. **474**, 47 (1997).
90. P. F. Scott, *et al*., *ibid*. **461**, L1 (1996).
91. E. M. Leitch, A. C. S. Readhead, T. J. Pearson, S. T. Myers, S. Gulkis, *ibid*., in press (available at http://xxx.lanl.gov/abs/astro-ph/9807312).
92. G. Jungman, M. Kamionkowski, A. Kosowsky, D. Spergel, *Phys. Rev. D* **54**, 1332 (1996).
93. For the current status of parameter estimation from CMB data, see J. R. Bond and A. H. Jaffe, available at http://xxx.lanl.gov/abs/astro-ph/9809043.
94. R. L. Davis, H. M. Hodges, G. F. Smoot, P. J. Steinhardt, M. S. Turner, *Phys. Rev. Lett*. **69**, 1856 (1992).
95. U. Seljak and M. Zaldarriaga, *ibid*. **78**, 2054 (1997); *Phys. Rev. D* **55**, 1830 (1997).
96. M. Kamionkowski, A. Kosowsky, A. Stebbins, *Phys. Rev. Lett*. **78**, 2058 (1997); *Phys. Rev. D* **55**, 7368 (1997).
97. B. Sadoulet, *Rev. Mod. Phys*. **71S**, 197 (1999).
98. L. J. Rosenberg, *Proc. Natl. Acad. Sci. U.S.A*. **95**, 59 (1998).
99. G. Jungman, M. Kamionkowski, K. Griest, *Phys. Rep*. **267**, 195 (1996).
100. Y. Fukuda *et al*., Super-Kamionkande Collaboration, *Phys. Rev. Lett*. **81**, 1562 (1998).
101. P. J. Steinhardt, L. Wang, I. Zlatev, available at http://xxx.lanl.gov/abs/astro-ph/9812313; I. Zlatev, L. Wang, P. J. Steinhardt, available at http://xxx.lanl.gov/abs/astro-ph/9807002.
102. We thank R. Caldwell, R. Cen, X. Fan, G. Huey, P. J. E. Peebles, L. Wang, and members of the SCP team for their contributions and collaborations on work described here. Supported by NSF grant AST93-15368 (N.A.B., Princeton); U.S. Department of Energy (DOE) grant DE-FG02-91ER40671 (P.J.S., Princeton); the Physics Division, E. O. Lawrence Berkeley National Laboratory of the U.S. DOE under contract DE-AC03-76SF000098; and the NSF's Center for Particle Astrophysics, University of California, Berkeley, under grant ADT-88909616 (S.P.).

REVIEW: EXPERIMENTAL ASTROPHYSICS

Modeling Astrophysical Phenomena in the Laboratory with Intense Lasers

Bruce A. Remington,[1] David Arnett,[2] R. Paul Drake,[3] Hideaki Takabe[4]

Astrophysical research has traditionally been divided into observations and theoretical modeling or a combination of both. A component sometimes missing has been the ability to quantitatively test the observations and models in an experimental setting where the initial and final states are well characterized. Intense lasers are now being used to recreate aspects of astrophysical phenomena in the laboratory, allowing the creation of experimental test beds where observations and models can be quantitatively compared with laboratory data. Experiments are under development at intense laser facilities to test and refine our understanding of phenomena such as supernovae, supernova remnants, gamma-ray bursts, and giant planets.

Modern intense lasers produce energy densities in submillimeter-scale volumes that are far larger than those produced by any other method. With these highly versatile laser facilities, matter can be prepared reproducibly in conditions that are equivalent, in a rigorously scaled sense, to those in large astrophysical systems such as supernovae, Herbig-Haro jets, or giant planets. Examples of areas that can be studied include strong shock phenomena, high–Mach number jets, strongly coupled plasmas, compressible hydrodynamic instabilities, radiation flow, photoevaporation front hydrodynamics, and fundamental properties such as opacities and equations of state (EOS).

Nuclear fusion reactions are the fundamental energy source of stars, and their cross sections quantify the individual reaction probabilities, allowing the heat production inside stars to be calculated. Opacities are the fundamental atomic properties that govern radiation transport within stars. Opacities quantify the probability that an atom will absorb photons that pass within its vicinity and consequently control to a large extent the temperature profiles of the interiors of stars. These fundamental "input" quantities—cross sections and opacities—are required in models of phenomena such as stellar pulsations and supernova light curves. The research reviewed here is aimed at probing astrophysical dynamics directly—the "output" of the models—by creating scaled reproductions of the astrophysical systems in the laboratory.

[1]Lawrence Livermore National Laboratory, L021, Livermore, CA, 94550, USA. E-mail: remington2@llnl.gov [2]Steward Observatory, University of Arizona, Tucson, AZ, 85721, USA. E-mail: darnett@as.arizona.edu [3]Atmospheric, Oceanic, and Space Sciences, University of Michigan, 2455 Hayward Street, Ann Arbor, MI, 48109–2143, USA. E-mail: rpdrake@umich.edu [4]Institute of Laser Engineering, Osaka University, Yamada-Oka 2-6, Shita, Osaka 565, Japan. E-mail:takabe@ile.asaka-u.ac.jp

Supernovae

Core-collapse supernovae (SNe) represent the dramatic endpoint in the life cycle of a star (*1*–*5*). The final death throes of the star are spent in a high-stakes "tug of war" pitting quantum mechanical degeneracy pressure against gravitational pressure. The outcome determines whether the final state is a white dwarf, neutron star, or black hole and is based on the strength of the degeneracy pressure to withstand the radially inward tug of gravity (*6*). Stars with initial masses of 1 to 8 $M_\odot$ (where $M_\odot$ corresponds to the mass of the sun) finish their hydrogen burning while their cores are not yet degenerate. They undergo core contraction, which raises the core density and temperature sufficiently to trigger He burning. These stars subsequently lose mass effectively and end their lifetimes as white dwarfs, with masses of $\sim$0.6 $M_\odot$. White dwarfs are supported by the pressure of the degenerate electrons in their interiors; that is, it is the quantum mechanical Pauli exclusion principle that prevents further collapse. The maximum mass possible for a white dwarf is the Chandrashekar limiting mass, $M_{Ch} \approx 1.4\ M_\odot$. More massive stars have high enough temperatures in their cores to continue the nuclear fusion burning cycle up to Fe. Once the core reaches Fe, the nuclear fusion reactions no longer release net energy (because the nuclear binding energy per nucleon is maximum in Fe, at nearly 9 MeV per nucleon), and the thermonuclear fires are extinguished. The mass of the Fe core continues to grow as the surrounding layers burn their way to this thermonuclear end point until the Fe core mass